CHEMPHYSCHEM

DOI: 10.1002/cphc.201100514

Basic Principles for Rational Design of High-Performance Nanostructured Silicon-Based Thermoelectric Materials

Chun Cheng Yang*[b] and Sean Li[a]

Recently, nanostructured silicon-based thermoelectric materials have drawn great attention owing to their excellent thermoelectric performance in the temperature range around 450 °C, which is eminently applicable for concentrated solar thermal technology. In this work, a unified nanothermodynamic model is developed to investigate the predominant factors that determine the lattice thermal conductivity of nanocrystalline, nanoporous, and nanostructured bulk Si. A systematic study shows that the thermoelectric performance of these materials can be substantially enhanced by the following three basic principles: 1) artificial manipulation and optimization of roughness with surface/interface patterning/engineering; 2) grain-size reduction with innovative fabrication techniques in a controllable fashion; and 3) optimization of material parameters, such as bulk solid–vapor transition entropy, bulk vibrational entropy, dimensionality, and porosity, to decrease the lattice thermal conductivity. These principles may be used to rationally design novel nanostructured Si-based thermoelectric materials for renewable energy applications.

1. Introduction

High-efficiency thermoelectric (TE) materials have the potential to contribute to significant reductions in both greenhouse gas emissions and the world's dependence on fossil fuels, owing to their unique capability of interconverting temperature gradients and electricity on a solid-state basis.[1–4] Generally, the performance of a TE material is determined by the dimensionless figure of merit $ZT = S^2\sigma T/\kappa$, where S, σ, T, and κ are Seebeck coefficient, electrical conductivity, absolute temperature, and thermal conductivity, respectively.[5] In addition, κ is composed of an electronic contribution κ_E and a lattice or phonon contribution κ_L ($\kappa = \kappa_E + \kappa_L$). In semiconductors, thermal transport is dominated by phonons, whereas electrons generally play a minor role, as $\kappa_E \ll \kappa_L$.[6] Thus, the thermal conductivity discussed in this work refers to κ_L. Due to the interdependency of the above parameters, their optimization required for high-performance TE materials with high ZT has been a challenge over the past half century.

Recently, minimizing κ_L in Si-based materials through nanostructuring technology has attracted intensive interest due to their potential application in TE devices.[7–10] It is known that bulk Si is a poor TE material with $ZT \approx 0.01$ at 300 K[11] because of its high thermal conductivity ($\kappa_L \approx 150\ W\,m^{-1}\,K^{-1}$ at room temperature[12]). However, the κ_L of nanostructured Si can be greatly reduced to near the amorphous limit associated with strong phonon scattering, which is caused by the increase in surfaces or interfaces through nanotechnology. For example, 100-fold decrease of κ_L in Si nanowires over that of bulk Si has been reported recently, resulting in $ZT = 0.6$ at room temperature.[8] This has triggered enormous research efforts to develop novel nanostructured Si-based TE materials. More recently, nanostructuring bulk materials has emerged as an effective approach to decouple electrical and thermal transport parameters, and led to an unprecedented increase in TE performance over the state-of-the-art TE materials.[13] The p-type nanostructured bulk SiGe alloys show a ZT of 0.95 at 1173–1223 K, which is about 90% higher than what is currently used in space-voyage missions.[14] A ZT of 0.7 at 1275 K has also been reported for n-type nanostructured bulk Si, which is a factor of 3.5 larger than that of heavily doped single-crystal Si.[15] In these nanocomposites, the κ_L value is minimized by enhancing the interfacial phonon scattering while the electron transport is preserved, contributing to higher ZT. Moreover, nanoporous Si with randomly distributed pores also exhibits ultralow κ_L (even lower than $0.1\ W\,m^{-1}\,K^{-1}$) at room temperature, which is three orders of magnitude smaller than that of its fully dense bulk counterpart.[16,17] This could lead to an enhancement in ZT and make nanoporous Si highly appealing for TE applications.

In complement to experiments, a number of theoretical methods[18–21] have also been developed to study the origin of size- and dimensionality-dependent $\kappa_L(r,d)$ in Si-based nanomaterials, where r is the radius of nanoparticles and nanowires or the half-thickness of thin films, and the dimensionality $d = 0$ for nanoparticles, $d = 1$ for nanowires, and $d = 2$ for thin films. However, to date, systematic investigation of κ_L of nanostructured Si-based TE materials and nanocrystalline, nanoporous, and nanostructured bulk Si is very limited. The intrinsic factor

[a] Prof. S. Li
School of Materials Science and Engineering
The University of New South Wales
NSW 2052 (Australia)

[b] Dr. C. C. Yang
Centre for Advanced Materials Technology (CAMT)
School of Aerospace, Mechanical and Mechatronic Engineering J07
The University of Sydney, Sydney, NSW 2006, Australia
Fax: (+61) 2-93517060
E-mail: chuncheng.yang@sydney.edu.au

that dominates the variation of κ_L on the nanometer scale remains unclear. Moreover, a better understanding of the fundamentals of phonon transport and the enhancement of energy conversion efficiency in nanocrystals, nanopores, and nanocomposites is desirable. In this work, a unified nanothermodynamic model is developed to study the underlying mechanism behind the size-dependent κ_L of the aforementioned Si-based TE materials, and thus provide new insights for rational design of novel TE materials for scale-up applications.

2. Methodology

2.1. Nanocrystalline Si

On the basis of a kinetic theory, κ_L of a bulk crystal is given by $\kappa_L = C\nu_s\lambda/3$, where C is the heat capacity, ν_s the average phonon velocity, and λ the phonon mean free path.[5] Note that the size effect on C is negligible.[19] Thus, we only need to consider the size dependences of ν_s and λ to derive the size-dependent κ_L. Recently, we found that the size- and dimensionality-dependent cohesive energy $E_c(r,d)$ determines the variation of the potential profile for nanocrystals, which is related to the crystallographic structures and the corresponding transition functions.[22] As a result, $E_c(r,d)$ dominates the size effect on a number of physicochemical properties in low-dimensional materials, including ν_s and λ.[20] On the basis of the approximation of an isotropic continuum, $\nu_s(\infty) \propto \Theta(\infty)$ can be obtained, where ∞ denotes the bulk and Θ is the characteristic Debye temperature.[23] At a certain temperature, $\lambda(\infty) = 20aT_m(\infty)/(\gamma^2 T)$, resulting in $\lambda(\infty) \propto T_m(\infty)$, where a is the lattice constant, $T_m(\infty)$ the bulk melting temperature, and γ the Gruneisen constant.[24] As $\Theta^2(\infty) \propto T_m(\infty) \propto E_c(\infty)$,[22] we have $\nu_s(\infty) \propto E_c^{1/2}(\infty)$ and $\lambda(\infty) \propto E_c(\infty)$. It is assumed that these bulk relationships can be extended to the nanometer scale as a first-order approximation.[22] In this case, with the developed $E_c(r,d)$ function,[25] a nanothermodynamic model can be established to calculate κ_L of semiconductor nanocrystals, which is expressed as Equation (1)

$$\kappa_L(q,d,r)/\kappa_L(\infty) = q\exp\left(-\frac{\lambda}{2r}\right)\left[\left(1-\frac{1}{12r/r_0-1}\right)\exp\left(-\frac{2S_b}{3R}\frac{1}{12r/r_0-1}\right)\right]^{3/2} \quad (1)$$

where $\kappa_L(q,d,r)$ is the lattice thermal conductivity of nanocrystals and $\kappa_L(\infty)$ the corresponding bulk counterpart, $r_0 = (3-d)h$ denotes a critical size at which all atoms of the nanocrystal are located on its surface with h being the atomic diameter, S_b is the bulk solid–vapor transition entropy of crystals, and R is the ideal gas constant. The term $q\exp[-\lambda/(2r)]$ was incorporated into Equation (1) to characterize the interface scattering, where q is a specular scattering parameter ($q=0$ for fully diffuse interface, $q=1$ for fully specular interface, and $0<q<1$ for partially specular and partially diffuse interfaces).[19,20] Since the size effect on λ has been considered in the discussion above, it is assumed to be a constant in the term $q\exp[-\lambda/(2r)]$. Moreover, the parameter q depends greatly on fabrication methods of nanostructures. Note that $0<q\leq 1$ in Equation (1)[19,20] and our model suffers from a limitation in its description of $\kappa_L(q,d,r)$ when $q=0$, which is related to the Casimir limit.[26] Further theoretical efforts will be directed towards this issue. From Equation (1), it can be seen that $\kappa_L(q,d,r) = \kappa_L(\infty)$ when both $r=\infty$ and $q=1$. This indicates that in the case of fully specular scattering ($q=1$), $\kappa_L(q,d,r) = \kappa_L(\infty)$ for bulk materials, whereas $\kappa_L(q,d,r) < \kappa_L(\infty)$ for nanocrystals. The origin of this difference is due to the intrinsic phonon confinement effect (e.g., size-dependent ν_s and λ), which results in different phonon dispersion in nanocrystals compared with the corresponding bulk counterparts, especially when the crystal size approaches the phonon mean free path. This is in agreement with reported experimental data and other theoretical analyses in the literature.[27]

2.2. Nanoporous Si

Nanoporous Si is a topologically connected and three-dimensional structure, whereby the pore is considered to be a vacant space among Si particles.[21] Thus, $d=0$ and r is the mean radius of Si nanocrystallites here. The porosity p is defined as the ratio of the pore volume to the total volume. Compared with Si nanocrystals, further reduction in κ_L has been observed in experiments on nanoporous Si due to the porous nature of the structure.[16,17] This is because the propagation of lattice vibrations is terminated at the edges of voids in the porous structure, and this impedes thermal transport significantly. To account for this reduction of κ_L in nanoporous Si, two simplified models have been developed on the basis of Fourier heat conduction theory: the R model derived by Russell[28] and the E model derived by Eucken.[29] As a result, similar to Equation (1), the κ_L of nanoporous Si can be described by Equations (2.1) and (2.2) for R and E models, respectively.

$$\kappa_L(q,d,r,p)/\kappa_L(q,d,r) = (1-p^{2/3})/(1-p^{2/3}+p) \quad (2.1)$$

$$\kappa_L(q,d,r,p)/\kappa_L(q,d,r) = (1-p)/(1+p/2) \quad (2.2)$$

2.3. Nanostructured Bulk Si

For nanostructured bulk Si, the inclusions are Si nanograins.[15] Thus, $d=0$ and r is the average grain radius here. It is known that the size effect in the isolated nanoparticles originates from their increased surface/volume ratio, whereas numerous grain boundaries dominate in the nanostructured bulk materials.[30] Thus, the κ_L values in nanoparticles and nanocomposites are different due to their distinct surface (interface) states. The size-dependent physicochemical properties of nanocomposites can be modeled by introducing an additional parameter $\beta = 1/\{1+[2S_{vib}/(3R)+1][\gamma_{sv}(\infty)/\gamma_{gb}(\infty)-1]\}$ into Equation (1) to characterize the difference between surfaces and grain boundaries, where S_{vib} denotes the bulk vibrational entropy and $\gamma_{sv}(\infty)$ and $\gamma_{gb}(\infty)$ are surface energy and grain boundary energy, respectively.[30,31] In this case, from Equation (1), $\kappa_L(q,r)/\kappa_L(\infty)$ of the

nanocomposites is given by Equation (3).

$$\kappa_L(q,r)/\kappa_L(\infty) = q\exp\left(-\frac{\lambda}{2r}\right)\left[\left(1-\frac{1}{4r/h-1}\right)\exp\left(-\frac{2\beta S_b}{3R}\frac{1}{4r/h-1}\right)\right]^{3/2} \quad (3)$$

3. Results and Discussion

Figure 1 plots the results calculated from Equation (1) and the recent reported experimental data of $\kappa_L(q,d,r)/\kappa_L(\infty)$ for rough Si nanowires with $d=1$. The parameters used in the modeling were $\lambda=40.9$ nm,[32] $h=0.2352$ nm,[33] $S_b=E_b/T_b=144\ J\,mol^{-1}\,K^{-1}$ with $E_b=456\ kJ\,mol^{-1}$ and $T_b=3173$ K.[33] Our

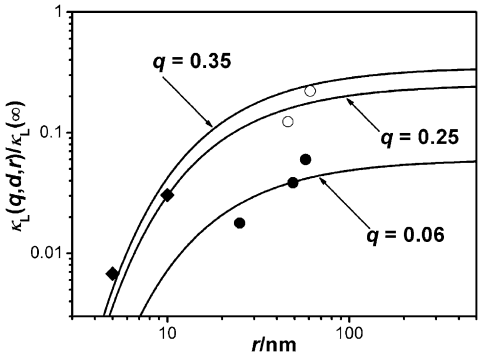

Figure 1. $\kappa_L(q,d,r)/\kappa_L(\infty)$ of rough Si nanowires with $d=1$. The solid lines denote model predictions calculated from Equation (1) with different q values. The symbols ●,[8] ◆,[9] and ○[10] are experimental data.

results are in good agreement with the experimental data, and the developed model describes the κ_L trend precisely even on the deep nanometer scale. It is discernable that $\kappa_L(q,d,r)$ can be remarkably reduced (by 1–2 orders of magnitude) by boundary scattering when the size of Si nanowires is smaller than the phonon mean free path. On the other hand, electron transport will not be significantly affected, since the material size is larger than the mean free path of electrons or holes. This is the major mechanism behind the enhancement of *ZT* in low-dimensional TE materials in which phonon movement is restricted without hindering electron motion. In Equation (1), $q\exp[-\lambda/(2r)]$ is much smaller than the latter term due to larger λ value of Si (40.9 nm), which shows that the interface scattering effect dominants while the intrinsic size effect on v_s and λ also contributes to the reduction of κ_L.[20] Moreover, from Figure 1, $\kappa_L(q,d,r)$ decreases with decreasing q, and an ultralow κ_L can be achieved for $q=0.06$, corresponding to very rough surfaces/interfaces of Si nanowires as reported recently.[8] It implies that the surface/interface roughness plays an important role in determining the phonon transport in TE materials at the nanometer scale. In this case, the high performance of Si-based thermoelectric materials with high *ZT* value can be developed by artificial manipulation of roughness by surface engineering and grain size reduction at nanometer scale. This may lead to a development in the design and optimization of surface/interface patterns/structures to enhance the properties of low-dimensional thermoelectric materials.

Figures 2 and 3 plot the results calculated from Equations (1) and (2) as well as the experimental data of $\kappa_L(q,d,r,p)$ for nano-

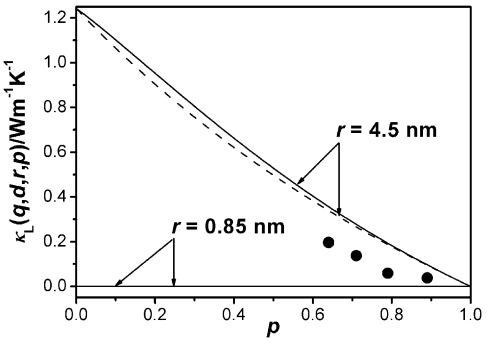

Figure 2. $\kappa_L(q,d,r,p)$ of nanoporous Si with r in the range of 0.85–4.5 nm and $q\approx1$ due to the porous nature. The solid and dashed lines denote model predictions calculated from Equations (2.1) and (2.2), respectively. Note that the solid and dashed lines almost coincide with each other for $r=0.85$ nm. The symbols ● are experimental data.[16]

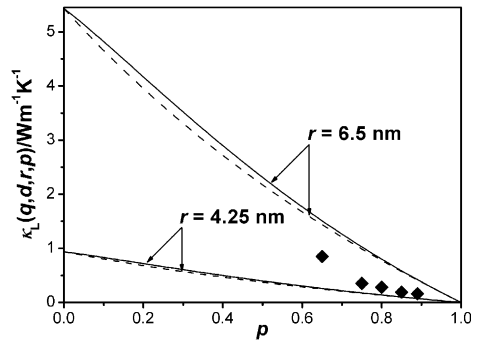

Figure 3. $\kappa_L(q,d,r,p)$ of nanoporous Si with r in the range of 4.25–6.5 nm and $q\approx1$ due to the porous nature. The solid and dashed lines denote model predictions calculated from Equations (2.1) and (2.2), respectively. The symbols ◆ are experimental data.[17]

porous Si with $q\approx1$ due to porous nature of the structures. Note that the measured r values are in size ranges of 0.85–4.5 and 4.25–6.5 nm in the experiments.[16,17] For comparison, we also calculate ranges of $\kappa_L(q,d,r,p)$ values of nanoporous Si, as shown in the figures. The $\kappa_L(q,d,r,p)$ value decreases with increasing p, and all experimental data are located in the calculated value ranges, which demonstrates the accuracy of the developed model. From the figures, we also find that the difference between the R [Eq. (2.1)] and E [Eq. (2.2)] models is negligible. Thus, both of these models can be used to calculate the porosity effect on κ_L in porous materials. Moreover, nanoporous Si exhibits extremely low κ_L values (0.0378–0.85 $W\,m^{-1}\,K^{-1}$), which are near or even below the amorphous limit (the so-called minimum thermal conductivity of 0.2–0.5 $W\,m^{-1}\,K^{-1}$).[4] This is beneficial for enhancement of *ZT* and possible application of nanoporous Si in TE devices. Although the electronic structure of nanoporous Si with random pore arrangement is substantially deteriorated, resulting in very low σ

and *ZT* at room temperature,[34] a significant improvement in σ can be achieved by ordering the nanopores periodically. This has been evidenced by recent theoretical results based on classical molecular dynamics and ab initio density functional theory.[21,35] As a result, additional improvements through further optimization of size and periodical arrangement of nanoscale pores, as well as impurity-doping level, are essential for developing high-performance TE materials based on nanoporous Si.

Figure 4 plots the results calculated from Equation (3) and an experimental datum of $\kappa_L(q,r)/\kappa_L(\infty)$ for nanostructured bulk Si. The parameter β used in Equation (3) is determined as follows: for Si, $S_{vib} = 6.7\ J\,mol^{-1}\,K^{-1}$ and $\gamma_{sv}(\infty) = 0.765\ J\,m^{-2}$ are cited from the open literature,[36] while $\gamma_{gb}(\infty)$ can be calculated by $\gamma_{gb}(\infty) = 4hS_{vib}H_m(T)/3V_mR$, where $H_m(T)$ is the temperature-dependent melting enthalpy, and V_m the molar volume of the crystal.[36] At room temperature, $H_m(T) = \Delta H_m/4$, where $\Delta H_m = 50.55\ kJ\,mol^{-1}$ is the bulk molar melting enthalpy and $V_m = 12.06\ cm^3\,mol^{-1}$.[36] Thus, $\gamma_{gb}(\infty) = 0.265\ J\,m^{-2}$ and $\beta = 0.256$ can be obtained. As shown in the figure, the agreement between our calculated result and the experimental datum is achieved by fitting a specular scattering parameter q to $q = 0.07$, where $\kappa_L(q,r)$ sharply decreases with decreasing r at nanometer scale due to large interface/volume ratio of the Si nanocomposites. The high-density internal interfaces in the nanocomposites could scatter phonons effectively, reducing κ_L significantly.[15] This implies that periodic structures, such as superlattices, are not necessary for κ_L reduction. On the other hand, it is possible to cause dramatic differences in electronic density of states due to the quantum confinement effect and distortion of band structure by deliberate impurity doping in the TE nanocomposites.[37] These two routes have been demonstrated to be generally applicable to enhance the power factor $S^2\sigma$ in TE materials. As a result, a high *ZT* could be achieved in nanostructured bulk Si with fine grain size fabricated by innovative techniques, for example, electrostatic atomization or high-energy ball milling in a controllable fashion, followed by spark plasma sintering for a short duration with crystal growth control. Moreover, the best experimental value of $\kappa_L(q,d,r) = 6.2\ W\,m^{-1}\,K^{-1}$ (◆[15] in Figure 4) to date for nanostructured bulk Si is similar to that of bulk SiGe alloys, for example, $\kappa_L \approx 10\ W\,m^{-1}\,K^{-1}$ for $Si_{0.7}Ge_{0.3}$.[5] As a result, high-*ZT* nanostructured bulk Si, without the presence of expensive, rare, and heavy Ge, may become a very promising material for use in radioisotope TE generators in mass-constrained deep-space missions, replacing the state-of-the-art SiGe alloys.

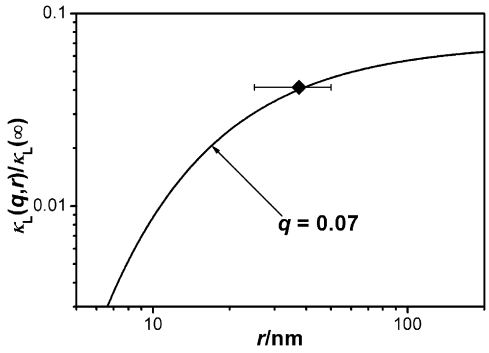

Figure 4. $\kappa_L(q,r)/\kappa_L(\infty)$ of nanostructured bulk Si. The solid line denotes the model prediction calculated from Equation (3). The symbol ◆ is an experimental datum.[15]

Figure 5 compares $\kappa_L(q,d,r,p)/\kappa_L(\infty)$ for Si nanoparticles, nanoporous Si, and nanostructured bulk Si, calculated from Equations (1), (2.2), and (3), respectively. As noted above, the calculation results from Equations (2.1) and (2.2) are very similar. Thus, only Equation (2.2) is used here. From Equations (2.1) and (2.2), it is evident that $\kappa_L(q,d,r,p)/\kappa_L(q,d,r) < 1$ for both R and E models, and thus smaller κ_L values of nanoporous Si compared with Si nanoparticles result for the same q, d, and r. This can be clearly seen from Figure 5, where $p = 0.5$ for nanoporous Si is used as an example. In this case, nanoporous Si with aligned pores is more attractive for TE application than Si nanowires. Moreover, the nanoporous Si may provide a few advantages over Si nanowires in fabrication, doping, and power factor enhancement due to the energy-filtering effect. From the figure, we also find that the result calculated from Equation (3) is only slightly larger than that of Equation (1) in the full range of sizes for the same q and d. This is due to their similar mechanisms of reduction of thermal conductivity dominated by the boundary scattering effect, while the minor difference is caused by the parameter β, where $\beta < 1$ is expected since $\gamma_{sv}(\infty) > \gamma_{gb}(\infty)$. This indicates that fully dense Si nanocomposites with fine grain size could show comparable κ_L to rough Si nanowires. Moreover, the Si nanocomposites can solve the critical challenges appearing in Si nanowires, for example, poor thermal stability and mechanical properties, interdiffusion, and high cost. In fact, these challenges have impeded their application for power regeneration at high temperature. On the other hand, the nanocomposite TE materials show great potential for scale-up applications because they can be produced in large quantities and in a form that is compatible with existing TE device configurations.

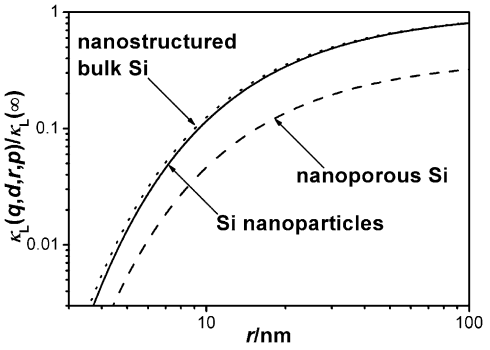

Figure 5. Comparisons of $\kappa_L(q,d,r,p)/\kappa_L(\infty)$ for Si nanoparticles, nanoporous Si, and nanostructured bulk Si calculated from Equations (1) (——), (2.2) (-----), and (3) (••••), respectively, with $q = 1$, $d = 0$, and $p = 0.5$.

From Equations (1) and (3), we find that a lower $\kappa_L(q,d,r)$ can be obtained for the materials with larger S_b, r_0, or β due to the intrinsic size effect on ν_s and λ. Since $\beta = 1/\{1+[2S_{vib}/$

$(3R)+1][\gamma_{sv}(\infty)/\gamma_{gb}(\infty)-1]\}$, smaller S_{vib} and $\gamma_{sv}(\infty)/\gamma_{gb}(\infty)$ values could lead to a larger β. As a result, on the one hand, it is possible to search for novel thermoelectric semiconductors with larger S_b and smaller S_{vib}. On the other hand, it offers a new avenue to achieve high energy-conversion efficiency, at least low lattice thermal conductivity, by controlling $\gamma_{sv}(\infty)/\gamma_{gb}(\infty)$ through surface or grain boundary engineering. As $r_0=(3-d)h$, changing d also results in different $\kappa_L(q,d,r)$ in the nanocrystals for the same q and r. This is ascribed to the various dimensionalities of confinement and thus different phonon dispersion relations. The $\kappa_L(q,d,r)$ values calculated from Equation (1) are smaller for nanoparticles than for nanowires, thin films, or superlattices, since the phonon dispersion in the nanoparticles with large surface/volume ratio is more pronounced. In this case, engineering zero-dimensional semiconductor nanomaterials, nanoporous and nanostructured bulk materials, and so on, shows potential to address the critical issues of achieving high *ZT*.

From the systematic investigation and discussions above, three basic principles are developed for rational design of novel nanostructured thermoelectric materials: 1) artificial manipulation and optimization of roughness by surface/interface patterning/engineering; 2) grain-size reduction with innovative fabrication techniques in a controllable fashion; and 3) optimization of material parameters, bulk solid–vapor transition entropy, bulk vibrational entropy, dimensionality, porosity, and so on, to decrease the lattice thermal conductivity. Based on the aforementioned principles, nanoporous and nanostructured bulk Si play a crucial role in developing high-efficiency low-cost TE materials and further in addressing critical energetic and climatic issues that the community is facing today.

3. Conclusion

The origin of size-dependent lattice thermal conductivity of nanocrystalline, nanoporous, and nanostructured bulk Si was investigated systematically through establishment of a unified nanothermodynamic model. It was found that 1) the lattice thermal conductivity can be remarkably reduced by 1–2 orders of magnitude through the boundary scattering effect and intrinsic size effect in these nanomaterials; 2) nanoporous Si exhibits smaller lattice thermal conductivity than rough Si nanowires due to the porosity effect; 3) fully dense Si nanocomposites with fine grain size have comparable lattice thermal conductivity to rough Si nanowires; 4) periodic structures, such as superlattices, are not necessary for reduction of thermal conductivity; and 5) high-performance nanostructured bulk Si may become to a very promising material in radioisotope thermoelectric generators for deep-space missions, replacing the state-of-the-art SiGe alloys. On the basis of these results, three basic principles have been concluded for rational design of novel nanostructured thermoelectric materials. Considering the simplicity of fabrication, doping, power-factor enhancement, scale-up application, and so on, nanoporous and nanostructured bulk Si show enormous potential for the development of high-efficiency low-cost TE materials, and thus addressing critical energetic and climatic issues we are facing.

Acknowledgements

This project is financially supported by the Australian Research Council Discovery Program (Grant No. DP0880548).

Keywords: nanostructures · nanowires · silicon · thermodynamics · thermoelectric effect

[1] R. Venkatasubramanian, E. Siivola, T. Colpitts, B. O'Quinn, *Nature* **2001**, *413*, 597–602.
[2] A. Majumdar, *Science* **2004**, *303*, 777–778.
[3] L. E. Bell, *Science* **2008**, *321*, 1457–1461.
[4] G. J. Snyder, E. S. Toberer, *Nature Mater.* **2008**, *7*, 105–114.
[5] T. M. Tritt, M. A. Subramanian, *MRS Bull.* **2006**, *31*, 188–198.
[6] M. S. Toprak, C. Stiewe, D. Platzek, S. Williams, L. Bertini, E. Müller, C. Gatti, Y. Zhang, M. Rowe, M. Muhammed, *Adv. Funct. Mater.* **2004**, *14*, 1189–1196.
[7] D. Y. Li, Y. Y. Wu, P. Kim, L. Shi, P. D. Yang, A. Majumdar, *Appl. Phys. Lett.* **2003**, *83*, 2934–2936.
[8] A. I. Hochbaum, R. K. Chen, R. D. Delgado, W. J. Liang, E. C. Garnett, M. Najarian, A. Majumdar, P. D. Yang, *Nature* **2008**, *451*, 163–167.
[9] A. I. Boukai, Y. Bunimovich, J. Tahir-Kheli, J.-K. Yu, W. A. Goddard III, J. R. Heath, *Nature* **2008**, *451*, 168–171.
[10] H. Kim, I. Kim, H.-J. Choi, W. Kim, *Appl. Phys. Lett.* **2010**, *96*, 233106.
[11] L. Weber, E. Gmelin, *Appl. Phys. A* **1991**, *53*, 136–140.
[12] "Thermal Conductivity: Metallic Elements and Alloys": *Thermophysical Properties of Matter, Vol. 1* (Eds.: Y. S. Touloukian, R. W. Powell, C. Y. Ho, P. G. Klemens), IFI/Plenum, New York, **1970**, p. 339.
[13] M. G. Kanatzidis, *Chem. Mater.* **2010**, *22*, 648–659.
[14] G. Joshi, H. Lee, Y. C. Lan, X. W. Wang, G. H. Zhu, D. Z. Wang, R. W. Gould, D. C. Cuff, M. Y. Tang, M. S. Dresselhaus, G. Chen, Z. F. Ren, *Nano Lett.* **2008**, *8*, 4670–4674.
[15] S. K. Bux, R. G. Blair, P. K. Gogna, H. Lee, G. Chen, M. S. Dresselhaus, R. B. Kaner, J.-P. Fleurial, *Adv. Func. Mater.* **2009**, *19*, 2445–2452.
[16] G. Gesele, J. Linsmeier, V. Drach, J. Fricke, R. Arens-Fischer, *J. Phys. D* **1997**, *30*, 2911–2916.
[17] P. Chantrenne, V. Lysenko, *Phys. Rev. B* **2005**, *72*, 035318.
[18] Y. F. Chen, D. Y. Li, J. R. Lukes, A. Majumdar, *J. Heat Transfer* **2005**, *127*, 1129–1137.
[19] L. H. Liang, B. W. Li, *Phys. Rev. B* **2006**, *73*, 153303.
[20] C. C. Yang, J. Armellin, S. Li, *J. Phys. Chem. B* **2008**, *112*, 1482–1486.
[21] J.-H. Lee, G. A. Galli, J. C. Grossman, *Nano Lett.* **2008**, *8*, 3750–3754.
[22] C. C. Yang, S. Li, *Phys. Rev. B* **2007**, *75*, 165413.
[23] A. R. Regel', V. M. Glazov, *Semiconductors* **1995**, *29*, 405–417.
[24] G. Soyez, J. A. Eastman, L. J. Thompson, G.-R. Bai, P. M. Baldo, A. W. McCormick, R. J. DiMelfi, A. A. Elmustafa, M. F. Tambwe, D. S. Stone, *Appl. Phys. Lett.* **2000**, *77*, 1155–1157.
[25] C. C. Yang, S. Li, *J. Phys. Chem. C* **2008**, *112*, 2851–2856.
[26] H. B. G. Casimir, *Physica* **1938**, *5*, 495–500.
[27] J. Zou, A. Balandin, *J. Appl. Phys.* **2001**, *89*, 2932–2938 and references therein.
[28] H. W. Russell, *J. Am. Ceram. Soc.* **1935**, *18*, 1–5.
[29] A. Eucken, *Forsch. Geb. Ingenieurwes.* **1932**, *53*, 6–21.
[30] Y. F. Zhu, J. S. Lian, Q. Jiang, *J. Phys. Chem. C* **2009**, *113*, 16896–16900.
[31] C. C. Yang, S. Li, *J. Electron. Mater.* **2011**, *40*, 953–956.
[32] G. Chen, *Phys. Rev. B* **1998**, *57*, 14958–14973.
[33] http://www.webelements.com/Web Elements Periodic Table.
[34] A. Yamamoto, H. Takazawa, T. Ohta, *Proc. 18th Int. Conf. Thermoelectr.* **1999**, 428–431.
[35] J.-H. Lee, J. C. Grossman, J. Reed, G. Galli, *Appl. Phys. Lett.* **2007**, *91*, 223110.
[36] C. C. Yang, J. C. Li, Q. Jiang, *Solid State Commun.* **2004**, *129*, 437–441 and references therein.
[37] J. P. Heremans, V. Jovovic, E. S. Toberer, A. Saramat, K. Kurosaki, A. Charoenphakdee, S. Yamanaka, G. J. Snyder, *Science* **2008**, *321*, 554–557.

Received: July 5, 2011
Published online on October 20, 2011

